A phosphoproteomic approach reveals that PKD3 controls phenylalanine and tyrosine metabolism

Alexander E. Mayer[1,*], Angel Loza-Valdes[1,2,*], Werner Schmitz[3], Jonathan Trujillo Viera[1], Michael Leitges[4], Andreas Schlosser[1], & Grzegorz Sumara[1,2,§]

[1]Rudolf Virchow Center, Center for Integrative and Translational Bioimaging, University of Würzburg, 97080 Würzburg, Germany.

[2]Nencki Institute of Experimental Biology, Polish Academy of Sciences, 3 Pasteur Street, 02-093Warsaw, Poland

[3]Theodor Boveri Institute, Biocenter, University of Würzburg, 97074 Würzburg, Germany.

[4]Tier 1, Canada Research Chair in Cell Signaling and Translational Medicine, Division of BioMedical Sciences / Faculty of Medicine, Craig L Dobbin Genetics Research Centre, Memorial University of Newfoundland, Health Science Centre 300 Prince Philip Drive, St. John`s, Newfoundland, Canada A1B 3V6

*These authors contributed equally.

§ Correspondence should be addressed to Grzegorz Sumara - Nencki Institute of Experimental Biology, Polish Academy of Sciences, 3 Pasteur Street, 02-093 Warsaw, Poland, email: g.sumara@nencki.edu.pl

Summary

Members of the Protein Kinase D (PKD) family (PKD1, 2, and 3) integrate hormonal and nutritional inputs to regulate complex cellular metabolism. Despite the fact that a number of functions have been annotated to particular PKDs, their molecular targets are relatively poorly explored. PKD3 promotes insulin sensitivity and suppresses lipogenesis in the liver. However, its substrates are largely unknown. Here we applied proteomic approaches to determine PKD3 targets. We identified over three-hundred putative targets of PKD3. Among them phenylalanine hydroxylase (PAH). PAH catalyses the conversion of phenylalanine to tyrosine and its activity is regulated by, phenylalanine concentration and glucagon-induced signaling. Consistently, we showed that PKD3 is activated by glucagon and promotes tyrosine levels in primary hepatocytes and liver of mice.

Taken together, our comprehensive proteomic approach established that PKD3 determine the rate of phenylalanine to tyrosine conversion in the liver. Therefore, our data indicate that PKD3 might play a role in development of diseases related to the defective tyrosine and phenylalanine metabolism.

Key words: Protein Kinase D3 (PKD3), phenylalanine hydroxylase (PAH), phenylalanine (Phe), tyrosine (Tyr), Phenylketonuria (PKU), Hepatocytes, Glucagon

Introduction

Protein Kinase D (PKD) family members integrate multiple hormonal and metabolic signals to coordinate homeostasis of the organism (Kolczynska, Loza-Valdes et al., 2020, Löffler, Mayer et al., 2018, Mayer, Löffler et al., 2019, Rozengurt, 2011, Sumara, Formentini et al., 2009). The family of PKDs comprises three kinases: PKD1, PKD2, and PKD3 (Fu & Rubin, 2011, Rozengurt, 2011). PKDs share a basic structure composed of the cysteine-rich domain (CRD), essential for their affinity for their main activators phorbol esters and diacylglycerol (DAG). The pleckstrin homology domain (PH) and the c-terminal region determine the catalytic activity (Iglesias, Matthews et al., 1998, Rozengurt, Sinnett-Smith et al., 1997). PKD1 and PKD2 share the highest homology, while PKD3 kinase is the unique member of the family. PKD1 and PKD2 have been widely studied in different cellular processes such as trans-Golgi network dynamics, cell proliferation and cell migration, adipocytes function, insulin secretion as well as regulation of innate and adaptive immune cells function (Gehart, Goginashvili et al., 2012, Goginashvili, Zhang et al., 2015, Ittner, Block et al., 2012, Kolczynska et al., 2020, Löffler et al., 2018, Mayer et al., 2019, Rozengurt, 2011, Sumara et al., 2009, Zhang, Meszaros et al., 2017). The specific functions of PKD3 are still relatively unexplored. PKD3 has been implicated in tumor progression and invasiveness in breast and gastric cancers, as well as hepatocellular carcinoma (Huck, Duss et al., 2014, Yang, Xu et al., 2017, Zhang, Zhang et al., 2019). Furthermore, recent research has demonstrated that PKD3 regulates insulin sensitivity, lipid accumulation, and fibrogenesis in the liver (Mayer et al., 2019, Zhang, Liu et al., 2020). Thus, PKD3 plays a role in a wide range of cellular processes in both physiological and pathological conditions.

To date, only a few downstream targets of PKD3 have been identified. PKD3 phosphorylates G-protein-coupled receptor kinase-interacting protein 1 (GIT1) on serine 46 to regulate the localization of GIT1-paxilin complex and consequently cell shape and motility (Huck, Kemkemer et al., 2012). Moreover, ectopic expression of a constitutive active form of PKD3

(PKD3ca) in TNBC (triple-negative breast cancer cells) leads to hyperphosphorylation of S6 Kinase 1 (S6K1), a downstream target of the mechanistic target of rapamycin complex 1 (mTORC1), which is an energy sensor in the cell and sustains cell proliferation (Huck et al., 2014, Laplante & Sabatini, 2012). PKD3 also phosphorylates p65 at serine 536, a critical step for the upregulation of 6-phosphofructo-2-kinase/fructose-2,6-biphosphatase 3 (PFKFB3) and drives glycolysis in gastric cancer cells (Zhang et al., 2019). In addition, gain and loss of function studies suggest that PKD3 regulates the ERK1-MYC axis and promotes cell proliferation in cancer (Chen, Deng et al., 2008, Liu, Song et al., 2019). Finally, in hepatocytes, PKD3 suppresses insulin-dependent AKT and mTORC1/2 activation, which results in peripheral glucose intolerance and suppression of the hepatic lipid production (Mayer et al., 2019). Nevertheless, the PKD3 targets in the liver and other organs remain largely unexplored.

The liver has a major role in the regulation of glucose, lipid, and amino acids (AAs) homeostasis by regulating the adaptation to nutrient availability. In the liver, AAs are utilized to synthesize proteins and precursors for different bioactive molecules. Moreover, ammonia, a by-product of protein catabolism, is disposed as urea by the liver (Bröer & Bröer, 2017, Waterlow, 1999). Under certain physiological conditions such as fasting, the liver can utilize AAs to produce glucose or ketone bodies. This metabolic response is hormonally regulated by glucagon, which is released from the pancreatic alpha cells (Holst, Albrechtsen et al., 2017, Petersen, Vatner et al., 2017).

Phenylalanine (Phe) is an essential AA in mammals, and its conversion into tyrosine (Tyr) is crucial for the production of thyroid hormones and catecholamines. The conversion into tyrosine is tightly regulated by the enzyme phenylalanine hydroxylase (PAH), an enzyme that requires tetrahydrobiopterin (BH_4) as a cofactor, and molecular dioxygen as a substrate (Fitzpatrick, 1999, Kaufman, 1958). Mutations in PAH lead to phenylketonuria (PKU), an abnormal accumulation of Phe in peripheral tissues (Konecki & Lichter-Konecki, 1991,

Scriver, 2007, Williams, Mamotte et al., 2008). Of note, the expression of PAH is restricted to the liver and kidney, major organs involved in AAs metabolism (Hsieh & Berry, 1979). PAH activity is regulated allosterically by high intracellular levels of Phe and hormonally by glucagon and insulin. By contrast, it was recently shown that oxygen concentrations might affect PAH activity in hepatocytes due to oxygen zonation (Donlon & Kaufman, 1978b, Kaufman, 1958, Ying, Pey et al., 2010). Upon fasting, glucagon rewires liver metabolism and promotes AAs catabolism. Glucagon leads to an increase in cAMP (cyclic Adenosine Monophosphate) and activates protein kinase A (PKA), which phosphorylates PAH at serine 16 to promote its function and increase the rate of Phe to Tyr conversion (Miranda, Teigen et al., 2002).

Here we carried out a phosphoproteomic study to investigate phosphorylation events dependent on PKD3 and thus to identify putative PKD3 targets in the liver. We found over three hundred of putative substrates of PKD3, among them PAH. Consistently, in mice and primary hepatocytes overexpressing constitutive active form of PKD3 (PKD3ca), Tyr levels were elevated, while the deletion of PKD3 resulted in decreased conversion of Phe to Tyr. Moreover, we showed that glucagon signaling promotes PKD3 activation and PAH activity in hepatocytes. Finally, PKD3 is required for glucagon-induced Phe to Tyr conversion. Taken together, we have identified potential PKD3-specific substrates in hepatocytes and uncovered the function of PKD3 in the regulation of Phe and Tyr metabolism.

RESULTS

Unraveling putative targets of PKD3 in hepatocytes using substrate motif-specific antibodies

Previous research has delineated the role of PKD3 in the regulation of hepatic glucose and lipid metabolism (Mayer et al., 2019). However, the phosphorylation targets of PKD3 in the liver remain elusive. To unravel the putative targets of PKD3 in the liver we have utilized

primary hepatocytes derived from PKD3 knockout mice and transduced these cells with adenovirus to overexpress either EGFP or PKD3ca (Fig. 1A). Subsequently, protein lysates were isolated, and used for pull-down assays. For this, we utilized PKD substrate motif specific antibodies. PKD kinases recognize the consensus AAs motif sequence LxRxx[S*/T*] (where L – leucine, R – arginine, S – serine, T – threonine, and x – any AA) within their putative targets (Döppler, Storz et al., 2005, Franz-Wachtel, Eisler et al., 2012). Importantly, the arginine (R) in position -3 in relation to the phospho-acceptor is essential, whereas leucine (L) in -5 position might be in some cases replaced by other amino acids e.g. valine (V) or isoleucine (I) (Döppler et al., 2005). At first, phospho-(Ser/Thr) PKD substrate LxRxx[S*/T*] antibody was used for immunoprecipitation to enrich proteins that have a phosphorylated PKD motif in lysates from primary hepatocytes deficient for PKD3 expressing either EGFP control or PKD3ca (Fig. 1A). Overexpression of PKD3ca showed an increase in proteins with a PKD motif (Fig. 1B). Proteins with phosphorylated PKD motif were immunoprecipitated and characterized by mass spectrometry. 84 proteins were significantly enriched (significance of 1 or 2) in lysates from PKD3ca hepatocytes compared to the EGFP ones (Fig. 1C, D and Supplementary table 1). The protein with highest enrichment induced by PKD3ca was PKD3 itself, suggesting that PKD3 might be subjected to auto-phosphorylation. Although leucine in -5 position is frequently present in PKD motifs, other targets also have valine (V) or isoleucine (I) in -5 position (Döppler et al., 2005). Therefore, to complement our approach, we performed a similar experiment utilizing an antibody only partially specific for PKD motif Rxx[S*/T*]. Overexpression of PKD3ca led to an increase in proteins that have a phosphorylated Rxx[S*/T*] motif (Fig. 2A). Subsequently, proteins were immunoprecipitated, identified and quantified by mass spectrometry. 226 proteins were significantly enriched (significance of 1 or 2) in lysates from PKD3ca hepatocytes compared to the EGFP expressing ones (Fig. 2B, C and Supplementary table 3). Of note, using antibody against motif Rxx[S*/T*] we identified almost three times more putative targets of PKD3

compared to antibody against LxRxx[S*/T*] motif, suggesting that PKD3 can frequently phosphorylate imperfect consensus site.

Comparative analysis of putative PKD3 targets identified using antibodies against LxRxx[S*/T*] and Rxx[S*/T*] motifs

Our mass spectrometry screening identified 84 and 226 proteins significantly enriched using antibodies against LxRxx[S*/T*] and Rxx[S*/T*], respectively (Fig. 3A). Of note, 24 proteins were enriched in both screenings (Fig. 3A and C). In silico analysis revealed that 55% of proteins identified using antibody against LxRxx[S*/T*] motif, have at least one putative PKD consensus side resembling the sequence [L/V/I]xRxx[S*/T*]. Similarly, also 55% of proteins enriched from hepatocytes expressing PKD3ca using antibody against Rxx[S*/T*] had at least one [L/V/I]xRxx[S*/T*] motif in their sequence (Fig. 3B). 12 of the proteins which had in their sequence a [L/V/I]xRxx[S*/T*] motif, were enriched using both antibodies, against Rxx[S*/T*] and LxRxx[S*/T*] (Fig. 3B). In silico analysis also revealed that these 12 proteins have in total 30 putative PKD motifs. Further analysis of the 30 putative PKD motifs carried out in phosphosite.org repository showed that 11 sites of the motifs were previously reported. Noteworthy, 3 of the motifs were identified in the field of PKDs (also PKA signaling), namely LsRklS16 for phenylalanine hydroxylase (PAH), and LtRqkS3894 as well as LtRqlS5407 for dystonin (DST) (Fig. 3D). Moreover, a prediction tool for biological processes (ARCHS4) suggests that PKD3 signaling might influence catabolic and metabolic activity of PAH (Fig. 3E). PAH converts Phe to Tyr (Kaufman, 1958), therefore these data suggest that PKD3 might also regulate AAs metabolism in liver.

PKD3 signaling determines tyrosine levels in liver

To test whether PKD3 regulates PAH phosphorylation in hepatocytes, we transduced primary hepatocytes with increasing amounts of adenoviruses expressing either EGFP or PKD3ca. Subsequently, protein lysates were used to evaluate PAH migration on the SDS PAGE

followed by Western blotting. Interestingly, overexpression of PKDca leads to an upshift of PAH signal and appearance of the second band, which is specific for this protein. Interestingly, the upshift of PAH was more pronounced when hepatocytes were transduced with an increasing amount of PKD3ca (Fig. 4A). Furthermore, to explore the physiological role of PKD3 in Phe metabolism, we cultivated hepatocytes expressing either EGFP or PKD3ca in the medium deprived of Phe and Tyr. Following Phe/Tyr starvation, we supplemented the cell culture medium of hepatocytes with increasing amounts of Phe and determined the tyrosine levels in the cells. In the cells, which were not supplemented with Phe, expression of PKD3ca resulted in the most pronounced increase in Tyr levels compared to control hepatocytes. Supplementation of Phe in the medium resulted in increased concentrations of Tyr levels in control hepatocytes. However, at each of the tested conditions, Tyr levels were significantly higher in the cells expressing PKD3ca but not increasing further upon addition of Phe (Fig. 4B). This suggests that PKD3 promotes the conversion of Phe to Tyr in hepatocytes. To test whether PKD3 regulates levels of Tyr in the complex in vivo situation, we measured Tyr levels in mice expressing PKD3ca specifically in hepatocytes (Mayer et al., 2019). Of note, mice overexpressing PKD3ca presented higher levels of Tyr in hepatic extracts than corresponding control animals (Fig. 4C). Moreover, as revealed by metabolomics analysis, mice overexpressing PKD3ca presented also higher Tyr to Phe ratio compared to control animals, while the levels of other AAs were not altered (Fig. 4D and Supplementary table 2). Altogether, these results suggest that PKD3 has a key role in the conversion of Phe into Tyr in the liver.

A glucagon-PKD3 axis determines amino acid metabolism in the liver

Seminal papers in the early 1970s demonstrated that hepatic PAH activity is hormonally regulated by glucagon via PKA signaling (Abita, Milstien et al., 1976a, Donlon & Kaufman, 1978b). PKA phosphorylates Ser16 of PAH upon glucagon stimulation, which increases the

affinity of PAH for its main substrate, the amino acid Phe (Miranda et al., 2002). In addition, glucagon promotes formation of DAG, a well-known activator of PKD3 (Hermsdorf, Dettmer et al., 1989, L Rodgers, 2012). Glucagon is a classical hormone induced under fasting conditions that rewires metabolism in the liver primarily via PKA (Pilkis, Claus et al., 1988, Pilkis & Granner, 1992). Thus, in order to investigate whether glucagon also governs PKD activity and AAs metabolism, we starved primary hepatocytes from all AA for one hour, then cultured them in media containing either no amino acids (w/o AA), all amino acids (AA), all amino acids except Phe and Tyr (w/o Phe, Tyr), Phe exclusively, or Phe and Tyr exclusively for additional hour and stimulated them with glucagon for 5 or 20 minutes. Glucagon promotes phosphorylation of PKD3-Ser731/735 independent of amino acid stimulation. In addition, stimulation of primary hepatocytes with all AAs or with all AA except Phe and Tyr was sufficient to activate S6K-Thr389 as well as 4E-BP1-Thr37/46 and Ser65, which was reduced upon glucagon stimulation in a time-dependent manner after 5 and 20 min (Fig. 5A). Importantly, similarly to cells expressing PKD3ca, stimulation of hepatocytes with glucagon resulted in an upshift of PAH on the Western blot, probably resembling increased phosphorylation of this enzyme (Fig. 5A). All of these suggest that PKD3 might be required for glucagon-induced conversion of Phe to Tyr. Indeed, stimulation of primary control hepatocytes with glucagon resulted in increased Tyr levels, but in the cells-derived from PKD3-deficient mice, glucagon failed to increase Tyr levels (Fig. 5B). All of these data suggest that activation of PKD3 by glucagon is required for induction of Phe to Tyr conversion.

Discussion

Recent studies established PKD3 function in the regulation of hepatic lipid and glucose metabolism (Mayer et al., 2019). However, the direct targets of PKD3 in hepatic cells remained elusive. Utilizing proteomic approach on primary hepatocytes deficient for PKD3

and re-expressing PKD3ca we identified over three-hundred putative targets of PKD3. Importantly, this approach resulted in the identification of the novel function of PKD3 in the regulation of hepatic metabolism of AAs. Namely, we showed that PKD3 promotes the conversion of Phe to Tyr by activating PAH, a rate-limiting enzyme in this process.

In our studies, we utilized two complementary proteomic approaches. For pull-downs, we used two antibodies: against the full phospho-motif sequence of PKD LxRxx[S*/T*] and antibody against part of the PKD phospho-motif sequence Rxx[S*/T*]. Importantly, pull-downs using an antibody against part of the PKD motif revealed more of the potential targets of PKD3 than antibody against full sequence targeted by PKDs. This indicates that in a large number of PKD3 target proteins AA at the position -5 in relation to the phospho-acceptor AA might be other than leucine. Whether we used for pull-downs antibody against LxRxx[S*/T*] or Rxx[S*/T*] motif, almost 50% of identified proteins did not present in their sequence the consensus motif for PKDs. These might indicate that in our pull-downs we have also fished out proteins, which are interacting with the targets of PKD3 but are not phosphorylated by PKD3 themselves.

In total, 12 proteins were identified by both pull-downs and possess one or more PKD phosphorylation motifs in their sequence. Among them, we found PAH as a target for PKD3, which we confirmed by classical WB. In line with our findings, a computational analysis to predict gene functions suggests that PKD3 might be involved in phenylalanine metabolism. PAH has two putative PKD motifs (LsRklS16 and IpRpfS411). It was shown that Ser16 is phosphorylated upon glucagon stimulation via PKA activation (Abita, Milstien et al., 1976b, Donlon & Kaufman, 1978a). Furthermore, the classical PKA motif is RRx[S*/T*] and has in -2 position of Ser16 a lysine (K) and not arginine (R), which can also serve as a PKD motif (Pinna & Ruzzene, 1996). Therefore, it is plausible that glucagon also might affect hepatic PAH activity via PKD3 signaling leading to changes in Tyr concentration. Phosphorylation of

PAH on Ser16 increases the affinity of this enzyme to Phe (Arun, Kaddour-Djebbar et al., 2011, Doskeland, Martinez et al., 1996). Consistently, primary hepatocytes overexpressing PKD3ca presented higher levels of Tyr especially when cells were starved from Phe. Importantly, transgenic mice overexpressing PKD3ca had higher levels of Tyr in the liver as well as a higher Tyr to Phe ratio than littermate controls.

Canonical activation of PKA in the liver promotes amino acid catabolism (Holst et al., 2017). However, our findings suggest that glucagon also promotes the activation of PKD3 in primary hepatocytes independently of AA stimulation. Moreover, activation of PKD3 is required for the induction of conversion of Phe to Tyr by glucagon. All of these findings suggest that glucagon might act in liver also in a PKD3-dependent manner. Interestingly, our experiments provide a possible link between glucagon signaling and mTORC1 pathway since glucagon stimulation reduces drastically the activity of S6K-Thr389 as well as 4E-BP1-Thr37/46 and Ser65, which are crucial components of mTORC1.

As mentioned above, PKD3 regulates insulin signaling and lipogenesis in the liver by modulation of mTORC1, mTORC2, and AKT signaling (Mayer et al., 2019). Our current proteomic approach identified several potential targets of PKD3, which could explain the suppression of mTORC1, mTORC2, and AKT signaling by PKD3. For instance, Ral GTPase activating protein non-catalytic beta subunit (RalGAPβ), which can control mTORC1 activity in response to insulin stimulation (Chen, Leto et al., 2011, Martin, Chen et al., 2014) was the most enriched protein in the Rxx[S*/T*]-motif antibody-based pull-down. Moreover, Tuberous sclerosis (TSC) 1 and 2, which also control mTORC1 and mTORC2 activity (Ben-Sahra & Manning, 2017), were also found using our strategy to be a putative target of PKD3. Interestingly, the distal downstream target of mTORC2, NDRG1, was also found to be a putative target of PKD3. Since previous studies showed that NDRG1 promotes lipogenesis (Cai, El-Merahbi et al., 2017), this might also explain PKD3-dependent lipogenesis in the

liver. However, these putative targets of PKD3 require confirmation and the detailed functions of PKD3-dependent phosphorylation needs to be identified.

In different cancer cell types, GIT1, S6K1 and PFKFB3 have been identified as targets of PKD3 (Huck et al., 2014, Huck et al., 2012, Laplante & Sabatini, 2012, Zhang et al., 2019). However, these proteins did not appear in our pull-downs. This might indicate that in hepatocytes PKD3 phosphorylates different set of the proteins that in respective cancer cell types.

In summary, in our study we identified a plethora of putative targets for PKD3 in the liver. Among them PAH, which suggests that PKD3 plays a role in AAs metabolism. We confirmed that PKD3 promotes the conversion of Phe to Tyr in response to the glucagon stimulation. Moreover, we have identified numerous putative targets, which might suggest the role of PKD3 in the regulation of lipid metabolism or in insulin-dependent signaling.

Materials and Methods

Primary hepatocyte isolation, culture and infection

Primary mouse hepatocytes were prepared as described previously (Mayer et al., 2019). All relevant mouse models of PKD3-deficiency or overexpression were also described in (Mayer et al., 2019). All animal studies were approved by the local animal welfare authorities (Regierung von Unterfranken) with the animal protocol no. AK55.2-2531.01-124/13. All mouse primary hepatocytes were infected 4 to 6 hours after plating with adenoviruses expressing either enhanced green fluorescent protein (EGFP) (Ad-EGFP) or a constitutively active form of PKD3 (Ad-mycPKD3ca) at a multiplicity of infection (MOI) of 10. Medium was replaced the following morning, and cells were used for experiments 36 to 48 hours after infection. Transduction efficiency, which was 100%, was assessed by analyzing the expression of the EGFP reporter (which was present in all adenoviruses).

Phenylalanine conversion assay

Primary hepatocytes were fasted in DMEM without phenylalanine (Phe) and tyrosine (Tyr) for 1 h. Afterwards, cells were stimulated with either 0, 0.1 or 5 mM Phe for 1 h (500 µL/well, 12-well plate). Next, the cells were lysed in 120 µL lysis buffer followed by centrifugation at 10000*g* for 10 min at 4°C. Tyrosine was quantified using the Tyrosine Assay Kit (ABNOVA) according to the manufacturer's protocol.

Amino acids and glucagon stimulation

Primary hepatocytes were fasted in DMEM without AAs for 1 h. Then they were cultured with either no amino acids, with all amino acids, all amino acids except Phe and Tyr, with Phe exclusively, or Phe and Tyr exclusively for 1 h. DMEM without AA and DMEM without Phe and Tyr were supplemented with respective amounts of glucose, serine, glycine, Phe, and Tyr. Hepatocytes were stimulated with glucagon for 0, 5, and 20 min.

Immunoprecipitation (IP) and Western blot (WB) analysis

IP was performed on hepatocytes lysates using antibodies against LxRxx[S*/T*] and Rxx[S*/T*] phospho-motifs (both Cell Signaling) with Pierce Protein A/G Magnetic Beads according to the manufacturer's protocol. Briefly, 4 mg of protein (2 mg/mL) and 30 µg of antibody were used for each IP. Samples were eluted in 1x NuPAGE lithium dodecyl sulfate (LDS) sample buffer supplemented 60 mM DDT for 10 min at 95°C. Beads were magnetically separated from the immunoprecipitated product, which was further analyzed on WB or by Mass spectrometry.

Mass Spectrometry analysis

Gel electrophoresis and in-gel digestion were carried out according to the standard procedures.

An Orbitrap Fusion equipped with a PicoView ion source and coupled to an EASY-nLC 1000 were used for NanoLC-MS/MS analyzes.

MS and MS/MS scans were both obtained using an Orbitrap analyzer. The raw data was processed, analyzed, and quantified using the MaxQuant software. *Label-free quantification* (LFQ) intensities were used for protein quantification. Proteins with less than two identified razor and unique peptides were excluded. Data imputation was performed with values from a standard normal distribution with a mean of the 5% quantile of the combined log10-transformed LFQ intensities and a standard deviation of 0.1. Log2 transformed protein ratios of sample versus control with values outside a 1.5x (potential, significance 1) or 3x (extreme, significance 2) *interquartile range* (IQR), respectively, were considered as significantly enriched.

Metabolomics analysis (HPLC)

For AAs analysis, pieces of mouse liver were homogenized in 69 vol. methanol/H_2O (80/20, v/v) containing 3.5 µM lamivudine as external standard using an ultraturrax. The resulting

homogenate was centrifuged (2 min. max rpm) and 600 µl supernatant was applied to an activated and equilibrated RP18 SPE-column (activation with 1 ml acetonitrile and equilibration with 1 ml methanol/H_2O (80/20, v/v) (Phenomenex Strata C18-E, 55 µm, 50 mg/1 ml, Phenomenex Aschaffenburg, Germany). The resulting eluate was evaporated at room temperature using a vacuum concentrator. The evaporated samples were re-dissolved in 100 µl of 5 mM NH_4OAc in acetonitrile/ H_2O (25/75, v/v). The equipment used for LC/MS analysis was a Thermo Scientific Dionex Ultimate 3000 UHPLC system hyphenated with a Q Exactive mass spectrometer (QE-MS) equipped with a HESI probe (Thermo Scientific, Bremen, Germany). LC parameters: Mobile phase A consisted of 5 mM NH_4OAc in acetonitrile/H_2O (5/95, v/v), and mobile phase B consisted of 5 mM NH4OAc in acetonitrile/H_2O (95/5, v/v). Chromatographic separation of AAs was achieved by applying 3 µl of dissolved sample on a SeQuant ZIC-HILIC column (3.5 µm particles, 100 × 2.1 mm) (Merck, Darmstadt, Germany), combined with a Javelin particle filter (Thermo Scientific, Bremen, Germany) and a SeQuant ZIC-HILIC precolumn (5 µm particles, 20 × 2 mm) (Merck, Darmstadt, Germany) using a linear gradient of mobile phase A (5 mM NH_4OAc in acetonitrile/H_2O (5/95, v/v)) and mobile phase B (5 mM NH4OAc in acetonitrile/H_2O (95/5, v/v)). The LC gradient program was 100% solvent B for 2 min, followed by a linear decrease to 40% solvent B within 16 min, then maintaining 40% B for 6 min, then returning to 100% B in 1 min and 5 min 100% solvent B for column equilibration before each injection. The column temperature was set to 30 °C, the flow rate was maintained at 200 µL/min. The eluent was directed to the ESI source of the QE-MS from 1.85 min to 20.0 min after sample injection. MS Scan Parameters: Scan Type: Full MS, Scan Range: 69.0 - 1000 m/z, Resolution: 70,000, Polarity: Positive and Negative, alternating, AGC-Target: 3E6, Maximum Injection Time: 200 ms HESI Source Parameters: Sheath gas: 30, auxiliary gas: 10, sweep gas: 3, spray voltage: 2.5 kV in pos. mode and 3.6 kV in neg. mode, Capillary temperature: 320 °C, S-lens RF level: 55.0, Aux Gas Heater temperature: 120 °C. Data Evaluation: Peaks

corresponding to the calculated amino acid masses (MIM +/- H+ ± 2 mMU) were integrated using TraceFinder software (Thermo Scientific, Bremen, Germany). Alternatively, (for Fig. 4B and C and Fig. 5B) commercially available kit was used for Tyr quantification (Cell Biolabs - Biocat).

ACKNOWLEDGMENTS

We thank Dr. Olga Sumara for critical reading of our manuscript. This study was funded by European Research Council (ERC) Starting Grant SicMetabol (no. 678119), Emmy Noether grant Su 820/1-1 from the German Research Foundation, EMBO Installation Grant from European Molecular Biology Organization (EMBO), and the Dioscuri Centre of Scientific Excellence. The program was initiated by the Max Planck Society (MPG), managed jointly with the National Science Centre and mutually funded by the Ministry of Science and Higher Education (MNiSW) and the German Federal Ministry of Education and Research (BMBF).

REFERENCES

Abita J-P, Milstien S, Chang N, Kaufman S (1976a) In vitro activation of rat liver phenylalanine hydroxylase by phosphorylation. Journal of Biological Chemistry 251: 5310-5314

Abita JP, Milstien S, Chang N, Kaufman S (1976b) In vitro activation of rat liver phenylalanine hydroxylase by phosphorylation. J Biol Chem 251: 5310-4

Arun SN, Kaddour-Djebbar I, Shapiro BA, Bollag WB (2011) Ultraviolet B irradiation and activation of protein kinase D in primary mouse epidermal keratinocytes. Oncogene 30: 1586-96

Ben-Sahra I, Manning BD (2017) mTORC1 signaling and the metabolic control of cell growth. Current opinion in cell biology 45: 72-82

Bröer S, Bröer A (2017) Amino acid homeostasis and signalling in mammalian cells and organisms. Biochemical Journal 474: 1935-1963

Cai K, El-Merahbi R, Loeffler M, Mayer AE, Sumara G (2017) Ndrg1 promotes adipocyte differentiation and sustains their function. Scientific reports 7: 1-9

Chen J, Deng F, Singh SV, Wang QJ (2008) Protein kinase D3 (PKD3) contributes to prostate cancer cell growth and survival through a PKCε/PKD3 pathway downstream of Akt and ERK 1/2. Cancer research 68: 3844-3853

Chen X-W, Leto D, Xiong T, Yu G, Cheng A, Decker S, Saltiel AR (2011) A Ral GAP complex links PI 3-kinase/Akt signaling to RalA activation in insulin action. Molecular biology of the cell 22: 141-152

Donlon J, Kaufman S (1978a) Glucagon stimulation of rat hepatic phenylalanine hydroxylase through phosphorylation in vivo. J Biol Chem 253: 6657-9

Donlon J, Kaufman S (1978b) Glucagon stimulation of rat hepatic phenylalanine hydroxylase through phosphorylation in vivo. Journal of Biological Chemistry 253: 6657-6659

Döppler H, Storz P, Li J, Comb MJ, Toker A (2005) A phosphorylation state-specific antibody recognizes Hsp27, a novel substrate of protein kinase D. Journal of Biological Chemistry 280: 15013-15019

Doskeland AP, Martinez A, Knappskog PM, Flatmark T (1996) Phosphorylation of recombinant human phenylalanine hydroxylase: effect on catalytic activity, substrate activation and protection against non-specific cleavage of the fusion protein by restriction protease. Biochem J 313 (Pt 2): 409-14

Fitzpatrick PF (1999) Tetrahydropterin-dependent amino acid hydroxylases. Annual review of biochemistry 68: 355-381

Franz-Wachtel M, Eisler SA, Krug K, Wahl S, Carpy A, Nordheim A, Pfizenmaier K, Hausser A, Macek B (2012) Global detection of protein kinase D-dependent phosphorylation events in nocodazole-treated human cells. Molecular & Cellular Proteomics 11: 160-170

Fu Y, Rubin CS (2011) Protein kinase D: coupling extracellular stimuli to the regulation of cell physiology. EMBO reports 12: 785-796

Gehart H, Goginashvili A, Beck R, Morvan J, Erbs E, Formentini I, De Matteis MA, Schwab Y, Wieland FT, Ricci R (2012) The BAR domain protein Arfaptin-1 controls secretory granule biogenesis at the trans-Golgi network. Developmental cell 23: 756-768

Goginashvili A, Zhang Z, Erbs E, Spiegelhalter C, Kessler P, Mihlan M, Pasquier A, Krupina K, Schieber N, Cinque L (2015) Insulin secretory granules control autophagy in pancreatic β cells. Science 347: 878-882

Hermsdorf T, Dettmer D, Hofmann E (1989) Age-dependent effects of phorbol ester on adenylate cyclase stimulation by glucagon in liver of female rats. Biomedica biochimica acta 48: 255-260

Holst JJ, Albrechtsen NJW, Pedersen J, Knop FK (2017) Glucagon and amino acids are linked in a mutual feedback cycle: The liver–α-cell axis. Diabetes 66: 235-240

Hsieh MC, Berry HK (1979) Distribution of phenylalanine hydroxylase (EC 1.14. 3.1) in liver and kidney of vertebrates. Journal of Experimental Zoology 208: 161-167

Huck B, Duss S, Hausser A, Olayioye MA (2014) Elevated protein kinase D3 (PKD3) expression supports proliferation of triple-negative breast cancer cells and contributes to mTORC1-S6K1 pathway activation. Journal of Biological Chemistry 289: 3138-3147

Huck B, Kemkemer R, Franz-Wachtel M, Macek B, Hausser A, Olayioye MA (2012) GIT1 phosphorylation on serine 46 by PKD3 regulates paxillin trafficking and cellular protrusive activity. Journal of Biological Chemistry 287: 34604-34613

Iglesias T, Matthews S, Rozengurt E (1998) Dissimilar phorbol ester binding properties of the individual cysteine-rich motifs of protein kinase D. FEBS letters 437: 19-23

Ittner A, Block H, Reichel CA, Varjosalo M, Gehart H, Sumara G, Gstaiger M, Krombach F, Zarbock A, Ricci R (2012) Regulation of PTEN activity by p38δ-PKD1 signaling in neutrophils confers inflammatory responses in the lung. Journal of Experimental Medicine 209: 2229-2246

Kaufman S (1958) A new cofactor required for the enzymatic conversion of phenylalanine to tyrosine. Journal of Biological Chemistry 230: 931-939

Kolczynska K, Loza-Valdes A, Hawro I, Sumara G (2020) Diacylglycerol-evoked activation of PKC and PKD isoforms in regulation of glucose and lipid metabolism: a review. Lipids in Health and Disease 19: 1-15

Konecki DS, Lichter-Konecki U (1991) The phenylketonuria locus: current knowledge about alleles and mutations of the phenylalanine hydroxylase gene in various populations. Human genetics 87: 377-388

L Rodgers R (2012) Glucagon and cyclic AMP: time to turn the page? Current diabetes reviews 8: 362-381

Laplante M, Sabatini DM (2012) mTOR signaling in growth control and disease. Cell 149: 274-293

Liu Y, Song H, Yu S, Huang KH, Ma X, Zhou Y, Yu S, Zhang J, Chen L (2019) Protein Kinase D3 promotes the cell proliferation by activating the ERK1/c-MYC axis in breast cancer. Journal of Cellular and Molecular Medicine

Löffler MC, Mayer AE, Viera JT, Valdes AL, El-Merahbi R, Ade CP, Karwen T, Schmitz W, Slotta A, Erk M (2018) Protein kinase D1 deletion in adipocytes enhances energy dissipation and protects against adiposity. The EMBO journal 37

Martin TD, Chen X-W, Kaplan RE, Saltiel AR, Walker CL, Reiner DJ, Der CJ (2014) Ral and Rheb GTPase activating proteins integrate mTOR and GTPase signaling in aging, autophagy, and tumor cell invasion. Molecular cell 53: 209-220

Mayer AE, Löffler MC, Valdés AEL, Schmitz W, El-Merahbi R, Viera JT, Erk M, Zhang T, Braun U, Heikenwalder M (2019) The kinase PKD3 provides negative feedback on cholesterol and triglyceride synthesis by suppressing insulin signaling. Science signaling 12: eaav9150

Miranda FF, Teigen K, Thórólfsson M, Svebak RM, Knappskog PM, Flatmark T, Martınez A (2002) Phosphorylation and Mutations of Ser16 in Human Phenylalanine Hydroxylase KINETIC AND STRUCTURAL EFFECTS. Journal of Biological Chemistry 277: 40937-40943

Petersen MC, Vatner DF, Shulman GI (2017) Regulation of hepatic glucose metabolism in health and disease. Nature reviews endocrinology 13: 572

Pilkis S, Claus T, El-Maghrabi MR (1988) The role of cyclic AMP in rapid and long-term regulation of gluconeogenesis and glycolysis. Advances in second messenger and phosphoprotein research 22: 175-191

Pilkis SJ, Granner D (1992) Molecular physiology of the regulation of hepatic gluconeogenesis and glycolysis. Annual review of physiology 54: 885-909

Pinna LA, Ruzzene M (1996) How do protein kinases recognize their substrates? Biochim Biophys Acta 1314: 191-225

Rozengurt E (2011) Protein kinase D signaling: multiple biological functions in health and disease. Physiology 26: 23-33

Rozengurt E, Sinnett-Smith J, Zugaza J (1997) Protein kinase D: a novel target for diacylglycerol and phorbol esters. In Portland Press Ltd.

Scriver CR (2007) The PAH gene, phenylketonuria, and a paradigm shift. Human mutation 28: 831-845

Sumara G, Formentini I, Collins S, Sumara I, Windak R, Bodenmiller B, Ramracheya R, Caille D, Jiang H, Platt KA (2009) Regulation of PKD by the MAPK p38δ in insulin secretion and glucose homeostasis. Cell 136: 235-248

Waterlow J (1999) The mysteries of nitrogen balance. Nutrition research reviews 12: 25-54

Williams RA, Mamotte CD, Burnett JR (2008) Phenylketonuria: an inborn error of phenylalanine metabolism. The Clinical Biochemist Reviews 29: 31

Yang H, Xu M, Chi X, Yan Q, Wang Y, Xu W, Zhuang K, Li A, Liu S (2017) Higher PKD3 expression in hepatocellular carcinoma (HCC) tissues predicts poorer prognosis for HCC patients. Clinics and research in hepatology and gastroenterology 41: 554-563

Yefimenko I, Fresquet V, Marco-Marin C, Rubio V, Cervera J (2005) Understanding carbamoyl phosphate synthetase deficiency: impact of clinical mutations on enzyme functionality. J Mol Biol 349: 127-41

Ying M, Pey AL, Aarsæther N, Martinez A (2010) Phenylalanine hydroxylase expression in primary rat hepatocytes is modulated by oxygen concentration. Molecular genetics and metabolism 101: 279-281

Zhang J, Zhang Y, Wang J, Zhao Y, Ren H, Chu Y, Feng L, Wang C (2019) Protein kinase D3 promotes gastric cancer development through p65/6-phosphofructo-2-kinase/fructose-2, 6-biphosphatase 3 activation of glycolysis. Experimental cell research 380: 188-197

Zhang S, Liu H, Yin M, Pei X, Hausser A, Ishikawa E, Yamasaki S, Jin ZG (2020) Deletion of Protein Kinase D3 Promotes Liver Fibrosis in Mice. Hepatology

Zhang Z, Meszaros G, He W-t, Xu Y, de Fatima Magliarelli H, Mailly L, Mihlan M, Liu Y, Puig Gámez M, Goginashvili A (2017) Protein kinase D at the Golgi controls NLRP3 inflammasome activation. Journal of Experimental Medicine 214: 2671-2693

FIGURE LEGENDS

Figure 1: Identification of PKD3 substrates by immunoprecipitation using PKD substrate motif antibody LxRxx[S*/T*]. (A) Experimental design. Primary hepatocytes isolated from PKD3-deficient mice were transduced by adenovirus containing EGFP (controls) or the constitutive active form of PKD3 (PKD3ca). IP with PKD-substrate motif antibodies was performed on cell extracts and followed by mass spectrometry analysis. (B) WB analysis of protein lysates from PKD3-deficient primary hepatocytes transduced with either adenovirus expressing control EGFP (Ad-EGFP) or constitutive active PKD3 (Ad-mycPKD3ca) using PKD-substrate motif LxRxx[S*/T*]-specific antibody (n=3 independent experiments). (C) Scatter plot of the statistical significance of log2 transformed protein ratios versus log10-transformed LFQ intensities between control and PKD3ca expressing hepatocytes. Enriched proteins are indicated by red (2, significantly enriched) or green (1, potentially enriched) dots, blue ones are not enriched (0, not enriched). (D) 15 most enriched proteins identified by mass spectrometry showing number, UniProt accession number, gene names, protein names, peptide count in EGFP and PKD3ca samples, respectively, and log2 transformed LFQ protein ratio are shown in the table.

Figure 2: Identification of PKD3 targets in hepatocytes by IP with Rxx[S*/T*] antibody. (A) WB using Rxx[S*/T*] motif antibody on lysates from PKD3-deficient hepatocytes expressing control EGFP (Ad-EGFP) or constitutive active form of PKD3 (Ad-mycPKD3ca). (B) Scatter plot of the statistical significance of log2 transformed protein ratios versus log10-transformed LFQ intensities between control and PKD3ca expressing hepatocytes. Enriched proteins are indicated by red (2, significantly enriched) or green (1, potentially enriched) dots, blue ones are not enriched (0, not enriched). (C) 15 most enriched proteins identified by mass spectrometry in the experiment from C, showing number, UniProt accession number, gene names, protein names, peptide count in EGFP and PKD3ca samples, respectively, and log2 transformed LFQ protein ratio.

Figure 3: Comparative analysis of putative PKD3 targets identified using different motif antibodies. (A) Venn diagram of common putative substrates that were significantly enriched by both antibodies LxRxx[S*/T*] and Rxx[S*/T*]. (B) Computational identification of putative PKD motifs [L/V/I]xRxx[S*/T*] among putative substrates identified by both antibodies (percentage of proteins possessing a putative motif in brackets). Results were obtained using ExPASy ScanProsite tool. (C) List of 24 proteins enriched by both antibodies, LxRxx[S*/T*] and Rxx[S*/T*] with UniProt accession numbers, gene and protein names, peptide count and log2 transformed LFQ protein ratio for LxRxx[S*/T*] and Rxx[S*/T*] immunoprecipitations, respectively, and the amount of putative PKD motifs for each protein. (D) Flow of computational identification of putative PKD substrates by comparing the PKD motifs within proteins using phosphosite.org repository. (E) Prediction of biological processes potentially regulated by PKD3 using ARCHS[4].

Figure 4: PKD3 signaling controls PAH activity and determines cellular levels of Tyr. (A) PAH expression and shifting analyzed in hepatocytes transduced with increasing amounts of adenovirus expressing EGFP or PKD3ca at indicated MOIs using WB. (B) Phe to Tyr conversion assay in primary hepatocytes expressing either EGFP or PKD3ca. Cells were depleted from Phe and Tyr in the medium for 1 h before stimulation and incubated with 0, 0.1, or 5 mM Phe for 1 h. (C) Tyr levels in livers from control mice and mice overexpressing PKD3ca (n=12 and n=16). (D) Tyr to Phe ratio in liver tissues from control mice and mice overexpressing PKD3ca (n=12 and n=16).

Figure 5: A glucagon-PKD3 axis determines amino acids metabolism in the liver. (A) WB analysis of indicated proteins in primary hepatocytes deprived from all AA for one hour, then cultured in media containing either no amino acids (w/o AA), all amino acids (AA), all amino acids except Phe and Tyr (w/o Phe, Tyr), Phe exclusively, or Phe and Tyr exclusively for additional hour and stimulated with glucagon for 5 or 20 minutes. (B) Intracellular phenylalanine to tyrosine conversion assay in primary hepatocytes isolated from control or

PKD3-deficient mice and stimulated with glucagon for 20 minutes. Data are presented as mean ± SEM. *P>0.05, ***P>0.001 (one way ANOVA with post hoc Tukey's test).

Fig. 1

A

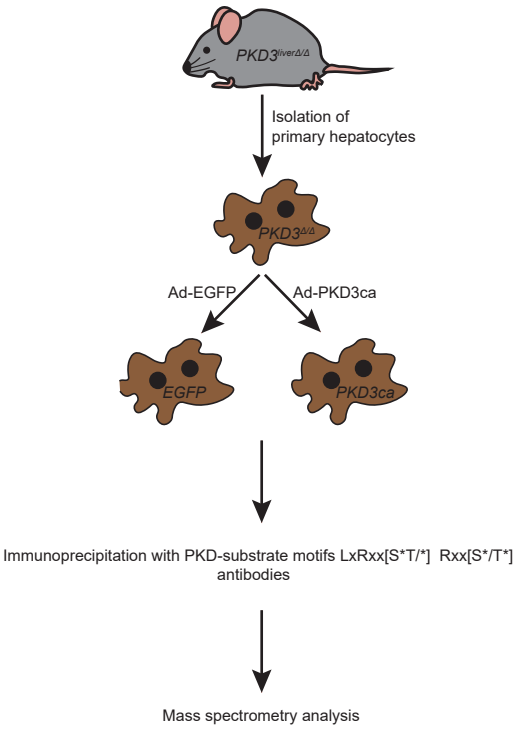

B

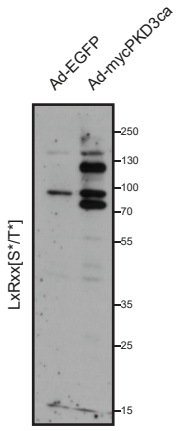

C

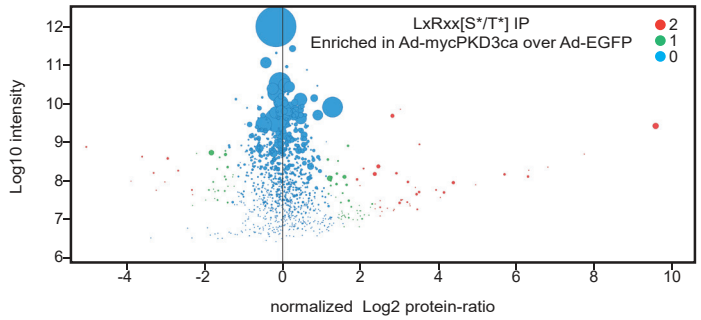

D

LxRxx[S*T/*]

No.	UniProt	Gene names	Protein names	Peptides Ad-EGFP	Peptides Ad-PKD3ca	Normalized Log2 protein-ratio
1	Q5FWX6	Prkd3	Serine/threonine-protein kinase D3	0	46	9.56
2	Q9JKP5	Mbnl1	Muscleblind-like protein1	1	2	7.73
3	Q3UIL6	Plekha7	Pleckstrin homology dom.-cont. fam. A member 7	1	3	6.79
4	Q8QZS1	Hibch	3-hydroxyisobutyryl-CoA hydrolase, mito.	1	3	6.31
5	P97861	Krt86	Keratin, type II cuticular Hb6	2	12	6.29
6	Q6A0A2	Larp4b	La-related protein 4B	1	13	5.68
7	P62984	Uba52	Ubiquitin-60S ribosomal protein L40	9	6	4.94
8	A2A7S8	Kiaa1522	Uncharacterized protein KIAA1522	3	20	4.37
9	F8VQB6	Myo10	Unconventional myosin-X	2	14	4.13
10	Q8BHL4	Gprc5a	Retinoic acid-induced protein 3	0	2	4.04
11	Q8K0Y2	Krt33a	Keratin, type I cuticular Ha3-I	2	6	3.93
12	P11352	Gpx1	Glutathione peroxidase 1	8	10	3.50
13	QSSZ5	Tns3	Tensin-3	1	12	3.50
14	Q05915	Gch1	GTP cyclohydrolase 1	2	7	3.45
15	Q3UJB9	Edc4	Enhancer of mRNA decapping protein 4	1	13	3.44

Fig. 2

A

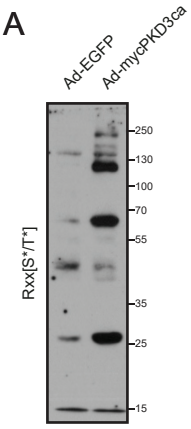

B

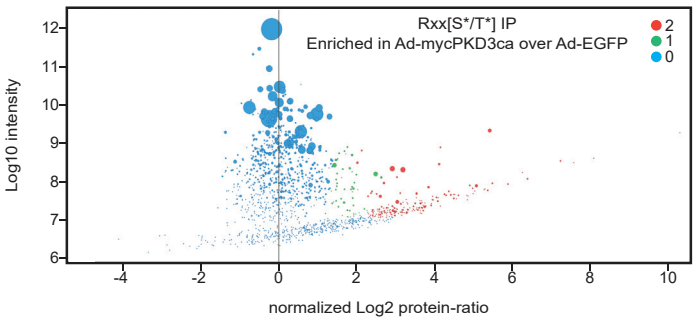

C

Rxx[S*T/*]

No.	UniProt	Gene names	Protein names	Peptides Ad-EGFP	Peptides Ad-PKD3ca	Normalized Log2 protein-ratio
1	Q8BQZ4	Ralgapb	Ral GTPase-activating protein subunit beta	1	3	10.24
2	P63260	Actg1	Actin, cyto. 2	48	44	8.04
3	Q9JKP5	Mbnl1	Muscleblind-like protein 1	1	2	7.53
4	P35700	Prdx1	Peroxiredoxin-1	3	11	7.19
5	K9J7B2	Ugta6b	UDP-glucuronosyltransferase	1	13	6.35
6	Q62426	Cstb	Cystatin-B	1	6	6.22
7	P70275	Sema3e	Semaphorin-3E	1	14	5.85
8	Q62266	Sprr1a	Cornifin-A	2	9	5.45
9	Q5FWX6	Prkd3	Serine/threonine-protein kinase D3	3	42	5.38
10	P54823	Ddx6	Probable ATP-depended RNA helicase DDX6	2	14	5.33
11	P63168	Dynll1	Dynein light chain 1, cyto.	0	3	5.26
12	P01887	B2m	Beta-2-microglobulin	1	2	5.24
13	Q80TV8	Clasp1	CLIP-associating protein 1	0	30	5.04
14	O54962	Banf1	barrier-to-autointegration factor	1	3	5.00
15	Q80U30	Clec16a	Protein CLEC16A	1	2	4.96

Fig. 3

A

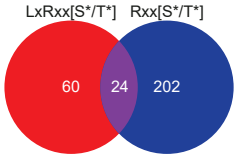

B

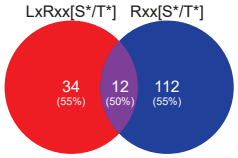

Hits with putative PKD substrate motif
[L/V/I]xRxx[S*/T*]

C

No.	UniProt	Gene names	Protein names	LxRxx[S*/T*] Peptides Ad-EGFP	LxRxx[S*/T*] Peptides Ad-PKD3ca	LxRxx[S*/T*] Normalized Log2 protein-ratio	Rxx[S*/T*] Peptides Ad-EGFP	Rxx[S*/T*] Peptides Ad-PKD3ca	Rxx[S*/T*] Normalized Log2 protein-ratio	Putative PKD motif
1	Q5FWX6	Pkd3	Serine/threonine-protein kinase D3	0	46	9.55	3	42	5.38	(1x)
2	Q9JKP5	Mbnl1	Muscleblind-like protein 1	1	2	7.73	1	2	7.53	
3	F8VQB6	Myo10	Unconventional myosin-X	2	14	4.13	0	24	3.72	(1x)
4	Q8BHL4	Gprc5a	Retionoic Acid-induced protein 3	0	2	4.03	0	3	4.46	(1x)
5	P11352	Gpx1	Glutathione peroxidase 1	8	10	3.50	4	12	4.13	
6	Q3UJB9	Edc4	Enhancer of mRNA-decapping protein 4	1	13	3.43	0	12	4.22	
7	P70275	Sema3e	Semaphorin-3E	4	11	3.21	1	14	5.85	
8	P13020	Gsn	Gelsolin	9	14	3.07	6	10	3.27	
9	Q8BQ30	Ppp1r18	Phostensin	5	15	2.91	4	23	4.09	(1x)
10	P35564	Canx	Calnexin	2	4	2.49	1	7	3.16	
11	Q61699	Hsph1	Heat shock protein 105 kDa	1	6	2.49	0	7	3.35	
12	Q91YU6	Lzts2	Leucine zipper putative tumor suppressor 2	1	4	2.36	0	8	3.64	
13	Q62266	Sprr1a	Cornifin-A	14	10	2.07	2	9	5.45	
14	P16331	Pah	Phenylalanine-4-hydroxylase	11	16	1.91	0	9	2.56	(2x)
15	P61967	Ap1s1	AP-1 complex subunit sigma-1A	1	2	1.97	0	3	2.31	
16	P09055	Itgb1	Integrin beta-1	2	3	1.92	1	5	3.11	
17	Q91VY9	Znf622	Zinc finger protein 622	2	2	1.91	0	8	3.43	(2x)
18	P20918	Plg	Plasminogen	3	14	1.64	2	12	4.39	(2x)
19	Q0VG62	1810022K09Rik	Uncharacterized protein C8orf59 homolog	2	2	1.52	1	2	2.95	(1x)
20	A0A087WQ89	2210011C24Rik	MCG5930	4	6	1.49	1	9	2.97	(1x)
21	Q8K2I2	Cchcr1	Coiled-coil alpha-helical rod protein 1	0	4	1.44	0	5	2.62	(2x)
22	P35700	Prdx1	Peroxiredoxin-1	7	10	1.41	3	11	7.19	(1x)
23	Q91YD6	Vill	Villin-like protein	8	12	1.24	7	14	1.49	
24	Q91ZU6	Dst	Dystonin	18	40	1.20	9	65	3.16	(15x)

D

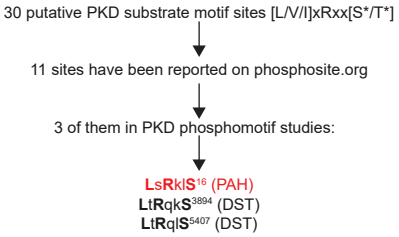

E

ARCHS[4] prediction for biological processes			
Rank	GO	Protein names	Z-score
1	0007506	gonadal mesoderm development	8.28
2	1902222	erythrose 4-phosphate/phosphoenolpyruvate family amino acid catabolic process	7.30
3	0006559	L-phenylalanine catabolic process	7.30
4	0051292	nuclear pore complex assembly	7.27
5	0006558	L-phenylalanine metabolic process	6.83

Fig. 4

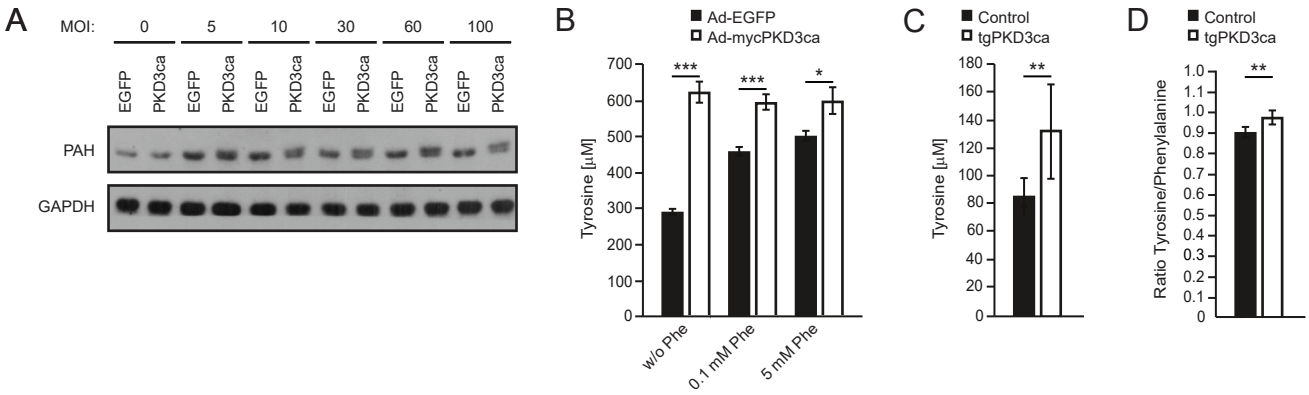
A
MOI:
0
5
10
30
60
100
EGFP
PKD3ca
PAH
GAPDH
B
Ad-EGFP
Ad-mycPKD3ca
Tyrosine [μM]
***
***
*
w/o Phe
0.1 mM Phe
5 mM Phe
C
Control
tgPKD3ca
Tyrosine [μM]
**
D
Control
tgPKD3ca
Ratio Tyrosine/Phenylalanine
**

Fig. 5

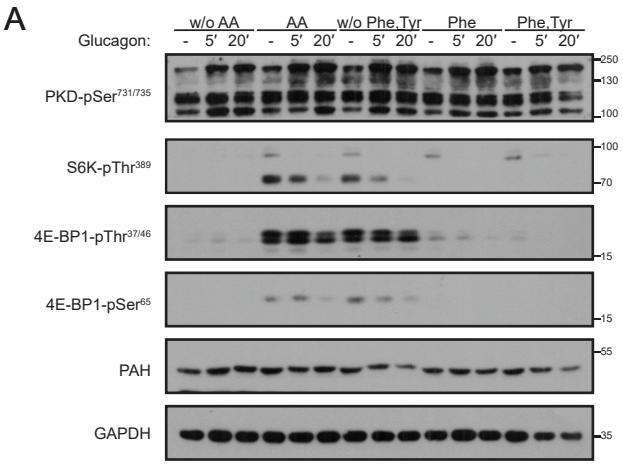
A
w/o AA
AA
w/o Phe,Tyr
Phe
Phe,Tyr
Glucagon:
- 5′ 20′ - 5′ 20′ - 5′ 20′ - 5′ 20′ - 5′ 20′
PKD-pSer731/735
S6K-pThr389
4E-BP1-pThr37/46
4E-BP1-pSer65
PAH
GAPDH
250
130
100
100
70
15
15
55
35

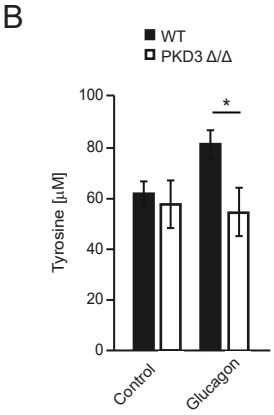
B
WT
PKD3 Δ/Δ
Tyrosine [µM]
100
80
60
40
20
0
*
Control
Glucagon

Supplementary Table 1

Proteins identified by MS from IP with LxRxx[S*/T*] antibody

Uniprot entry	Protein names	Gene names	Peptides EGFP	Peptides PKD3ca	norm.log2.Ratio. filt.LFQ.intensity	Sig.	Putative PKD substrate motifs
Q5FWX6	Serine/threonine-protein kinase D3	Prkd3	0	46	9,56	2	IlRvsS470
Q9JKP5	Muscleblind-like protein 1	Mbnl1	1	2	7,73	2	
Q3UIL6	Pleckstrin homology domain-containing family A member 7	Plekha7	1	3	6,79	2	IsRkyS229 VpRsiS562 LcResT766 LpReaT943 IiRhtS949 LeRlyS1060
Q8QZS1	3-hydroxyisobutyryl-CoA hydrolase, mitochondrial	Hibch	1	3	6,31	2	LsRvsS15
P97861	Keratin, type II cuticular Hb6	Krt86	2	12	6,29	2	
Q6A0A2	La-related protein 4B	Larp4b	1	13	5,68	2	IlReiS246 VdRlpS628
P62984	Ubiquitin-60S ribosomal protein L40	Uba52	9	6	4,94	2	
A2A7S8	Uncharacterized protein KIAA1522	Kiaa1522	3	20	4,37	2	IqRrgS136 LtRpmS261 LgRfsS337 LpRppT477 LrRalS838 LeRpvS909 VaRkpS952 LpRteS967
F8VQB6	Unconventional myosin-X	Myo10	2	14	4,13	2	IeRslS961
Q8BHL4	Retinoic acid-induced protein 3	Gprc5a	0	2	4,04	2	LpRqrS275
Q8K0Y2	Keratin, type I cuticular Ha3-I	Krt33a	2	6	3,93	2	
P11352	Glutathione peroxidase 1	Gpx1	8	10	3,50	2	
Q5SSZ5	Tensin 3	Tns3	1	12	3,50	2	LiRwdS332 LlRkpS571 VqRgiS648
Q05915	GTP cyclohydrolase 1	Gch1	2	7	3,45	2	
Q3UJB9	Enhancer of mRNA-decapping protein 4	Edc4	1	13	3,44	2	
P11370	Retrovirus-related Env polyprotein from Fv-4 locus	Fv4	2	3	3,40	2	LeRslT540
P17918	Proliferating cell nuclear antigen	Pcna	0	2	3,27	2	IcRdlS152
Q640L5	Coiled-coil domain-containing protein 18	Ccdc18	1	2	3,26	2	LeRnlS281 LdRllT695 LrRsiS1355
P70275	Semaphorin-3E	Sema3e	4	11	3,21	2	
Q9JJY4	Probable ATP-dependent RNA	Ddx20	3	6	3,19	2	IiRnyT618

Uniprot entry	Protein names	Gene names	Peptides EGFP	Peptides PKD3ca	norm.log2.Ratio. filt.LFQ.intensity	Sig.	Putative PKD substrate motifs
	helicase DDX20						
P13020	Gelsolin	Gsn	9	14	3,07	2	
P28740	Kinesin-like protein KIF2A	Kif2a	1	5	3,03	2	
E9QN70	Laminin subunit beta-1	Lamb1	2	2	3,02	2	LlRppS37
F6ZDS4	Nucleoprotein TPR	Tpr	0	14	2,99	2	LeRseT905 LqRasT1130 VeRpsT1881
Q8BQ30	Phostensin	Ppp1r18	5	15	2,91	2	LeRrsS126
O88487	Cytoplasmic dynein 1 intermediate chain 2	Dync1i2	3	4	2,86	2	VeRalS212
Q91YD3	mRNA-decapping enzyme 1A	Dcp1a	0	2	2,84	2	LyrnaS121 LpRnsT359 LeRkaS542
P35492	Histidine ammonia-lyase	Hal	21	25	2,81	2	LvRshS195
P28271	Cytoplasmic aconitate hydratase	Aco1	1	4	2,68	2	VmRfdT867
Q9CXI3	DBH-like monooxygenase protein 1	Moxd1	0	4	2,54	2	LtRcsS482 IyRpvT503
Q8QZY1	Eukaryotic translation initiation factor 3 subunit L	Eif3l	2	4	2,50	2	LlRlhS282 IqRtkS348
P35564	Calnexin	Canx	2	4	2,49	2	
Q61699	Heat shock protein 105 kDa	Hsph1	1	6	2,49	2	
Q8K2Q9	Shootin-1	Kiaa1598	4	24	2,46	2	
Q9D975	Sulfiredoxin-1	Srxn1	0	3	2,37	2	
Q91YU6	Leucine zipper putative tumor suppressor 2	Lzts2	1	4	2,36	2	
Q9QXL2	Kinesin-like protein KIF21A	Kif21a	5	26	2,36	2	LqRlqT739 VlRrkT829 VtRklS855 LeRrvT933 IsRqsS1231 LkRfqS1482
Q62266	Cornifin-A	Sprr1a	14	10	2,07	2	
Q6PEM6	GRAM domain-containing protein 3	Gramd3	4	2	1,98	2	LsRdsT219
P16331	Phenylalanine-4-hydroxylase	Pah	11	16	1,91	2	LsRklS16 IpRpfS411
Q9Z1Q9	Valine--tRNA ligase	Vars	4	9	2,29	1	
Q04750	DNA topoisomerase 1	Top1	5	4	2,25	1	
Q9CWY4	Gem-associated protein 7	Gemin7	0	2	2,21	1	
Q8K2D3	Enhancer of mRNA-decapping protein 3	Edc3	0	2	2,09	1	VyRriT262
P46062	Signal-induced proliferation-associated protein 1	Sipa1	0	6	2,04	1	LlRsgS53 LpRtlS903
Q91WK0	Leucine-rich repeat flightless-interacting protein 2	Lrrfip2	22	18	1,99	1	LlRstS151
Q91WT9	Cystathionine beta-synthase	Cbs	2	2	1,99	1	IvRtpT190

Uniprot entry	Protein names	Gene names	Peptides EGFP	Peptides PKD3ca	norm.log2.Ratio. filt.LFQ.intensity	Sig.	Putative PKD substrate motifs
P61967	AP-1 complex subunit sigma-1A	Ap1s1	1	2	1,98	1	
O35682	Myeloid-associated differentiation marker	Myadm	2	2	1,96	1	
Q3THS6	S-adenosylmethionine synthase isoform type-2	Mat2a	4	5	1,96	1	LrRngT172
Q8CGK3	Lon protease homolog, mitochondrial	Lonp1	5	4	1,93	1	
P09055	Integrin beta-1	Itgb1	2	3	1,92	1	
Q91VY9	Zinc finger protein 622	Znf622	2	2	1,91	1	LpRavT410 VqRmkS452
Q6IMF0	Keratin, type II cuticular Hb3	Krt83	2	13	1,81	1	
Q60953	Protein PML	Pml	3	7	1,76	1	LdRnhS227 LqRirT332 LaRnmS748
A2AN08	E3 ubiquitin-protein ligase UBR4	Ubr4	8	15	1,70	1	LnRldS950 LtRmtT1472 IvRenS1503 VkRtpS1732 LvRhaS1760 LtRlaS1945 IeRapS2364 VmRllS3057 LaRhnT4938
Q8VDJ3	Vigilin	Hdlbp	0	5	1,70	1	VaRlqT149 ViRgpS706
P84084	ADP-ribosylation factor 5	Arf5	3	4	1,68	1	
E9Q450	Tropomyosin alpha-1 chain	Tpm1	64	56	1,67	1	
P20918	Plasminogen	Plg	3	14	1,64	1	IpRctT264 LsRpaT678
P42125	Enoyl-CoA delta isomerase 1, mitochondrial	Eci1	4	4	1,61	1	
Q91XV3	Brain acid soluble protein 1	Basp1	1	3	1,59	1	
Q921U8	Smoothelin	Smtn	10	23	1,58	1	VtRlgS521 VqRstS798
Q9CQA6	Coiled-coil-helix-coiled-coil-helix domain-containing protein 1	Chchd1	1	2	1,58	1	
Q99NB9	Splicing factor 3B subunit 1	Sf3b1	2	2	1,57	1	
Q9DBJ3	Brain-specific angiogenesis inhibitor 1-associated protein 2-like protein 1	Baiap2l1	4	7	1,54	1	LqRsvS332
Q8CC35	Synaptopodin	Synpo	0	4	1,54	1	LgRstS134 LaRcpS740
Q91YW3	DnaJ homolog subfamily C member 3	Dnajc3	3	2	1,52	1	
Q0VG62	Uncharacterized protein C8orf59 homolog	1810022 K09Rik	2	2	1,52	1	VpRpeT34
P10648	N-terminally processed;Glutathione S-	Gsta2	3	6	1,51	1	

Uniprot entry	Protein names	Gene names	Peptides EGFP	Peptides PKD3ca	norm.log2.Ratio. filt.LFQ.intensity	Sig.	Putative PKD substrate motifs
	transferase A2						
Q62523	Zyxin	Zyx	0	2	1,50	1	
A0A087WQ89	MCG5930	2210011C24Rik	4	6	1,49	1	LsRpgS48
Q9D0R2	Threonine--tRNA ligase, cytoplasmic	Tars	0	3	1,44	1	
Q8K2I2	Coiled-coil alpha-helical rod protein 1	Cchcr1	0	4	1,44	1	VeRmsT401 VaRipS459
P35700	Peroxiredoxin-1	Prdx1	7	10	1,41	1	IlRqiT143
P07901	Heat shock protein HSP 90-alpha	Hsp90aa1	10	17	1,39	1	LlRyyT468
Q8VE19	WD repeat-containing protein mio	Mios	6	12	1,38	1	
Q9CQ22	Ragulator complex protein LAMTOR1	Lamtor1	4	4	1,36	1	
Q91YD6	Villin-like protein	Vill	8	12	1,25	1	
P99029	Peroxiredoxin-5, mitochondrial	Prdx5	6	5	1,23	1	VlRasT21
O70325	Phospholipid hydroperoxide glutathione peroxidase, mitochondrial	Gpx4	4	5	1,23	1	
Q91ZU6	Dystonin	Dst	18	40	1,21	1	LhRleS682 VaRkkS739 IqRkyS833 VeRwqS1272 LeRqdT1703 VlRpeS2146 LtRqkS3894 LtRskS4092 LlRslS4680 LdRakT5202 LtRqlS5407 LlRkqS5488 LeRaqS5759 VeRgrS6520 VpRagS7365
Q9D0I9	Arginine--tRNA ligase, cytoplasmic	Rars	5	7	1,18	1	IeRgeS336
Q91YR1	Twinfilin-1	Twf1	17	13	1,16	1	LfRldS75

Supplementary Table 2

Proteins identified by MS from IP with Rxx[S*/T*] antibody

Uniprot entry	Protein names	Gene names	Peptides EGFP	Peptides PKD3ca	norm.log2.Ratio. filt.LFQ.intensity	Sig.	Putative PKD substrate motifs
Q8BQZ4	Ral GTPase-activating protein subunit beta	Ralgapb	1	3	10,24	2	LaResS156 IsRprS357 InRdnS470 LvRgmS971
P63260	Actin, cytoplasmic 2	Actg1	48	44	8,04	2	
Q9JKP5	Muscleblind-like protein 1	Mbnl1	1	2	7,53	2	
P35700	Peroxiredoxin-1	Prdx1	3	11	7,19	2	IlRqiT143
K9J7B2	UDP-glucuronosyltransferase	Ugt1a6b	1	13	6,35	2	VpRfyT197 LkRdvS242 ImRlsS443
Q62426	Cystatin-B	Cstb	1	6	6,22	2	
P70275	Semaphorin-3E	Sema3e	1	14	5,85	2	
Q62266	Cornifin-A	Sprr1a	2	9	5,45	2	
Q5FWX6	Serine/threonine-protein kinase D3	Prkd3	3	42	5,38	2	IlRvsS470
P54823	Probable ATP-dependent RNA helicase DDX6	Ddx6	2	14	5,33	2	
P63168	Dynein light chain 1, cytoplasmic	Dynll1	0	3	5,26	2	
P01887	Beta-2-microglobulin	B2m	1	2	5,24	2	
Q80TV8	CLIP-associating protein 1	Clasp1	0	30	5,04	2	LeRhiS485 LnRplS568 LqRsrS600 LgRirT642 VsRiiT1026 IgRtpS1098 LrRsyS1159 ItRedS1333 IkRaqT1520
O54962	Barrier-to-autointegration factor	Banf1	1	3	5,00	2	
Q80U30	Protein CLEC16A	Clec16a	1	2	4,96	2	IlRqkS89
P12787	Cytochrome c oxidase subunit 5A, mitochondrial	Cox5a	0	3	4,95	2	
Q8VCH8	UBX domain-containing protein 4	Ubxn4	0	7	4,95	2	IeRrkT230 VkResT310 IwRliS428 IyRlrT487
P10810	Monocyte differentiation antigen CD14	Cd14	1	10	4,87	2	LkRvdT71 LdRnpS308
O09106	Histone deacetylase 1	Hdac1	0	8	4,83	2	VaRcwT313
Q9CXF4	TBC1 domain family member 15	Tbc1d15	0	3	4,81	2	
Q9CQQ7	ATP synthase F(0) complex	Atp5f1	2	7	4,80	2	

Uniprot entry	Protein names	Gene names	Peptides EGFP	Peptides PKD3ca	norm.log2.Ratio. filt.LFQ.intensity	Sig.	Putative PKD substrate motifs
	subunit B1, mitochondrial						
P27773	Protein disulfide-isomerase A3	Pdia3	1	11	4,58	2	LqReaT485
P62821	Ras-related protein Rab-1A	Rab1A	1	4	4,53	2	IdRyaS114
P09528	Ferritin heavy chain	Fth1	1	8	4,49	2	
Q9DBG1	Sterol 26-hydroxylase, mitochondrial	Cyp27a1	1	11	4,47	2	VsRdpS439
Q8K0D0	Cyclin-dependent kinase 17	Cdk17	0	4	4,47	2	LrRphS75 IhRriS137 LaRakS339
Q8BHL4	Retinoic acid-induced protein 3	Gprc5a	0	3	4,46	2	LpRqrS275
P20918	Plasminogen	Plg	2	12	4,39	2	IpRctT264 LsRpaT678
Q9R049	E3 ubiquitin-protein ligase AMFR	Amfr	0	12	4,34	2	LqRqrT642
Q05421	Cytochrome P450 2E1	Cyp2e1	1	15	4,27	2	
Q3UJB9	Enhancer of mRNA-decapping protein 4	Edc4	0	12	4,22	2	
Q91WT8	RNA-binding protein 47	Rbm47	2	7	4,13	2	VqRipT533
P11352	Glutathione peroxidase 1	Gpx1	4	12	4,13	2	
Q8BQ30	Phostensin	Ppp1r18	4	23	4,09	2	LeRrsS126
Q9DCX2	ATP synthase subunit d, mitochondrial	Atp5h	1	3	4,06	2	
Q64282	Interferon-induced protein with tetratricopeptide repeats 1	Ifit1	1	13	4,06	2	
Q8R084	UDP-glucuronosyltransferase	Ugt2b1	2	8	4,05	2	LgRptT246
P03975	IgE-binding protein	Iap	1	9	4,02	2	VsRkrS107
Q8VCW8	Acyl-CoA synthetase family member 2, mitochondrial	Acsf2	1	7	3,93	2	
V9GX76	Unconventional myosin-VI	Myo6	73	93	3,93	2	VlRylT169 LnRgcT279
Q8CHQ9	Probable N-acetyltransferase CML2	Cml2	2	7	3,92	2	
P61222	ATP-binding cassette sub-family E member 1	Abce1	1	5	3,91	2	
Q3TJZ6	Protein FAM98A	Fam98a	0	6	3,90	2	IlRtsS283
P14211	Calreticulin	Calr	1	10	3,88	2	
Q6PDK2	Histone-lysine N-methyltransferase 2D	Kmt2d	2	25	3,82	2	LgRagT424 VlRnlT1560 LdRipT1837 lsRgqT2695 VsRppS2962
Q9CY27	Very-long-chain enoyl-CoA reductase	Tecr	1	7	3,75	2	
Q02013	Aquaporin-1	Aqp1	1	3	3,75	2	LeRnqT44 LtnfS207
P62071	Ras-related protein R-Ras2	Rras2	1	7	3,73	2	
F8VQB6	Unconventional myosin-X	Myo10	0	24	3,72	2	IeRslS961

Uniprot entry	Protein names	Gene names	Peptides EGFP	Peptides PKD3ca	norm.log2.Ratio. filt.LFQ.intensity	Sig.	Putative PKD substrate motifs
P58660	Caspase recruitment domain-containing protein 10	Card10	4	9	3,68	2	VrRvlS629 VeRgsS1011
O88342	WD repeat-containing protein 1	Wdr1	1	3	3,68	2	VeRgvS20
Q91YN9	BAG family molecular chaperone regulator 2	Bag2	2	5	3,66	2	
Q99104	Unconventional myosin-Va	Myo5a	3	17	3,65	2	IrRaaT841
Q91YU6	Leucine zipper putative tumor suppressor 2	Lzts2	0	8	3,64	2	
P63242	Eukaryotic translation initiation factor 5A-1	Eif5a	1	3	3,64	2	
Q9CQW9	Interferon-induced transmembrane protein 3	Ifitm3	1	3	3,64	2	
Q922F4	Tubulin beta-6 chain	Tubb6	6	21	3,63	2	
Q8VCX1	3-oxo-5-beta-steroid 4-dehydrogenase	Akr1d1	1	2	3,61	2	
Q99KK2	N-acylneuraminate cytidylyltransferase	Cmas	0	12	3,61	2	LaRggS53 VhRrsS111
Q8BG80	F-box only protein 46	Fbxo46	0	8	3,61	2	LyRhvS453
Q61937	Nucleophosmin	Npm1	2	5	3,60	2	
Q9JLJ2	4-trimethylaminobutyraldehyde dehydrogenase	Aldh9a1	3	10	3,58	2	
P56593	Cytochrome P450 2A12	Cyp2a12	0	12	3,55	2	IpRriT373
P58137	Acyl-coenzyme A thioesterase 8	Acot8	1	4	3,52	2	VeRirT104
Q9JHU4	Cytoplasmic dynein 1 heavy chain 1	Dync1h1	4	20	3,52	2	IsRdlS387 IdRveT560 IdRqlT657 LpRiqS999 LeRerS1622 LaRlrS2382 IrRitT2521 VhRkyT2966 LeRmnT3008 LeRlfT4272 LpRswS4462
Q63886	UDP-glucuronosyltransferase 1-1	Ugt1a1	2	12	3,51	2	VkRdsS123 ImRlsS447
Q99K48	Non-POU domain-containing octamer-binding protein	Nono	3	7	3,50	2	
Q8BHD7	Polypyrimidine tract-binding protein 3	Ptbp3	2	11	3,48	2	
Q922P9	Putative oxidoreductase GLYR1	Glyr1	1	6	3,46	2	
A2AIX1	Protein transport protein sec16	Sec16a	0	17	3,44	2	LtRapS2101 LsRcsS2315
Q8BWS5	G protein-regulated inducer of neurite outgrowth 3	Gprin3	0	7	3,43	2	
Q91VY9	Zinc finger protein 622	Znf622	0	8	3,43	2	LpRavT410 VqRmkS452
Q3UMC0	Spermatogenesis-associated	Spata5	1	4	3,41	2	VeRgsS739

Uniprot entry	Protein names	Gene names	Peptides EGFP	Peptides PKD3ca	norm.log2.Ratio. filt.LFQ.intensity	Sig.	Putative PKD substrate motifs
	protein 5						
Q61699	Heat shock protein 105 kDa	Hsph1	0	7	3,35	2	
Q61495	Desmoglein-1-alpha	Dsg1a	2	2	3,31	2	VdRevT120 VfRpgS389 LqRtcT476
Q9D2G2	Dihydrolipoyllysine-residue succinyltransferase component of 2-OGDC, mitochondrial	Dlst	1	8	3,28	2	VsRafS13
Q5U465	Coiled-coil domain-containing protein 125	Ccdc125	0	8	3,28	2	VpRssS9 LkRscS492
P17182	Alpha-enolase	Eno1	1	9	3,28	2	
Q9CQF0	39S ribosomal protein L11, mitochondrial	Mrpl11	1	7	3,27	2	
P13020	Gelsolin	Gsn	6	10	3,27	2	
P26039	Talin-1	Tln1	1	10	3,26	2	LnRcvS1201
Q921G7	Electron transfer flavoprotein-ubiquinone oxidoreductase, mitochondrial	Etfdh	1	4	3,25	2	VnRnlS550
Q62186	Translocon-associated protein subunit delta	Ssr4	1	4	3,25	2	
O35632	Hyaluronidase-2	Hyal2	1	3	3,20	2	VyRqsS155 VrRnpS382
P09803	Cadherin-1	Cdh1	1	4	3,19	2	
P08226	Apolipoprotein E	Apoe	1	12	3,17	2	
Q91ZU6	Dystonin	Dst	9	65	3,16	2	LhRleS682 VaRkkS739 IqRkyS833 VeRwqS1272 LeRqdT1703 VlRpeS2146 LtRqkS3894 LtRskS4092 LlRslS4680 LdRakT5202 LtRqlS5407 LlRkqS5488 LeRaqS5759 VeRgrS6520 VpRagS7365
Q6PGG6	Guanine nucleotide-binding protein-like 3-like protein	Gnl3l	0	2	3,16	2	
P35564	Calnexin	Canx	1	7	3,16	2	
O35295	Transcriptional activator protein Pur-beta	Purb	1	8	3,14	2	
P34914	Bifunctional epoxide hydrolase 2	Ephx2	1	4	3,14	2	
Q8BGH2	Sorting and assembly machinery component 50 homolog	Samm50	0	8	3,14	2	LsRtaS243

Uniprot entry	Protein names	Gene names	Peptides EGFP	Peptides PKD3ca	norm.log2.Ratio. filt.LFQ.intensity	Sig.	Putative PKD substrate motifs
Q64433	10 kDa heat shock protein, mitochondrial	Hspe1	1	2	3,13	2	
Q61753	D-3-phosphoglycerate dehydrogenase	Phgdh	2	14	3,12	2	IvRsaT57 VgRagT78 LlReaS383
P09055	Integrin beta-1	Itgb1	1	5	3,11	2	
P53996	Cellular nucleic acid-binding protein	Cnbp	0	6	3,10	2	LaRecT173
Q9CQE8	UPF0568 protein C14orf166 homolog	RTRAF	0	6	3,09	2	
Q9Z2I8	Succinyl-CoA ligase [GDP-forming] subunit beta, mitochondrial	Suclg2	2	15	3,09	2	
Q9Z2I0	LETM1 and EF-hand domain-containing protein 1, mitochondrial	Letm1	0	5	3,05	2	LsRccT55
Q91VW5	Golgin subfamily A member 4	Golga4	9	48	3,02	2	LvRtsS119 LeRqrS891 LqRrlS1761
Q9JHI7	Exosome complex component RRP45	Exosc9	1	6	3,02	2	
P80316	T-complex protein 1 subunit epsilon	Cct5	4	12	3,01	2	
Q91YH5	Atlastin-3	Atl3	1	6	3,01	2	LiRdwS216
Q8K154	UDP-glucuronosyltransferase	Ugt2b34	1	7	3,01	2	LgRptT248
Q8R081	Heterogeneous nuclear ribonucleoprotein L	Hnrnpl	0	4	3,00	2	VdRaiT434 VkRptS528
A0A087WQ89	MCG5930	2210011C24Rik	1	9	2,97	2	LsRpgS48
Q61029	Lamina-associated polypeptide 2, isoforms beta/delta/epsilon/gamma	Tmpo	14	24	2,96	2	VgRkaT95 LtResT250
Q8CGC7	Bifunctional glutamate/proline--tRNA ligase;Glutamate--tRNA ligase;Proline--tRNA ligase	Eprs	0	9	2,96	2	LaRiaT63 LrRgmT467 IlRpwS1053
Q3UEP4	UDP-glucuronosyltransferase	Ugt2b36	1	6	2,96	2	VlRpsT60 LgRptT246
P32067	Lupus La protein homolog	Ssb	4	11	2,95	2	LnRltT63 IrRspS94
Q0VG62	Uncharacterized protein C8orf59 homolog	1810022K09Rik	1	2	2,95	2	VpRpeT34
E9Q5F4	Actin, cytoplasmic 1	Actb	30	31	2,94	2	
Q91ZA3	Propionyl-CoA carboxylase alpha chain, mitochondrial	Pcca	0	9	2,94	2	VsRslS48 ViRgvT475
P1063	Thioredoxin	Txn	1	3	2,92	2	
Q6VGS5	Protein Daple	Ccdc88c	0	19	2,91	2	LqRelS787 LiRqhS1184 VdRtdT1493 VsRsaS1792 LsRafS1798 LaRerT1848

Uniprot entry	Protein names	Gene names	Peptides EGFP	Peptides PKD3ca	norm.log2.Ratio. filt.LFQ.intensity	Sig.	Putative PKD substrate motifs
P24369	Peptidyl-prolyl cis-trans isomerase B	Ppib	0	5	2,90	2	
Q6ZWQ0	Nesprin-2	Syne2	12	67	2,90	2	IrRgrT968 LrRlmS1184 LaRlqT3013 IiRklS3097 LqRvrS3527 LsRtnS4096 VkRlyS4634 LhRlqT4927 IsRlvT5687 LqRwrT5743 IsRlqS5794 LaRieS6030 LlRqgT6489
Q8CGB3	Uveal autoantigen with coiled-coil domains and ankyrin repeats	Uaca	0	13	2,90	2	
Q9QUI0	Transforming protein RhoA	Rhoa	0	2	2,89	2	
P56391	Cytochrome c oxidase subunit 6B1	Cox6b1	1	2	2,88	2	
P14602	Heat shock protein beta-1	Hspb1	2	5	2,87	2	LlRspS15 LnRqlS86 IsRcfT143
Q791V5	Mitochondrial carrier homolog 2	Mtch2	1	5	2,86	2	
Q9DBF1	Alpha-aminoadipic semialdehyde dehydrogenase	Aldh7a1	3	9	2,85	2	LgRlvS133 VdRlrS352
Q3U0V1	Far upstream element-binding protein 2	Khsrp	2	7	2,84	2	
P97432	Next to BRCA1 gene 1 protein	Nbr1	0	2	2,82	2	LgRpeS351 ViRslT659
P52480	Pyruvate kinase PKM	Pkm	1	2	2,82	2	LvRasS403
A2AI08	Taperin	Tprn	2	8	2,82	2	VnRslS255
P68373	Tubulin alpha-1C chain	Tuba1c	7	18	2,80	2	LnRliS232
P10649	Glutathione S-transferase Mu 1	Gstm1	1	7	2,78	2	
Q9WU79	Proline dehydrogenase 1, mitochondrial	Prodh	1	6	2,78	2	
Q99PP6	Tripartite motif-containing protein 34A	Trim34a	2	8	2,77	2	LrRewS243
Q8BX02	KN motif and ankyrin repeat domain-containing protein 2	Kank2	0	4	2,76	2	
P53395	Lipoamide acyltransferase component of branched-chain alpha-keto acid dehydrogenase complex, mitochondrial	Dbt	1	10	2,75	2	VlRtwS11
P62835	Ras-related protein Rap-1A	Rap1a	1	4	2,74	2	
Q8JZN5	Acyl-CoA dehydrogenase family member 9,	Acad9	1	3	2,74	2	LsRgaT12 VlRefT28

Uniprot entry	Protein names	Gene names	Peptides EGFP	Peptides PKD3ca	norm.log2.Ratio. filt.LFQ.intensity	Sig.	Putative PKD substrate motifs
	mitochondrial						
Q8C052	Microtubule-associated protein 1S	Map1s	0	6	2,74	2	LrRllS324 LaRrsT659 LtRkpS831
P51658	Estradiol 17-beta-dehydrogenase 2	Hsd17b2	2	7	2,73	2	
P19536	Cytochrome c oxidase subunit 5B, mitochondrial	Cox5b	1	2	2,70	2	
Q9D6Y9	1,4-alpha-glucan-branching enzyme	Gbe1	1	7	2,69	2	
Q99MR8	Methylcrotonoyl-CoA carboxylase subunit alpha, mitochondrial	Mccc1	1	10	2,69	2	
Q61037	Tuberin	Tsc2	5	23	2,68	2	IlRelS49 LlRadS625 IyRcaS802 LvRrpT1203 LpRsnT1270 LhRsvS1291 IeRaiS1365
Q8QZY3	Developmental pluripotency-associated protein 3	Dppa3	0	8	2,68	2	
Q3TDQ1	Dolichyl-diphosphooligosaccharide--protein glycosyltransferase subunit STT3B	Stt3b	0	4	2,67	2	ViRfeS94
Q9R0Q7	Prostaglandin E synthase 3	Ptges3	0	2	2,64	2	
Q80U72	Protein scribble homolog	Scrib	1	10	2,63	2	LqRraT475 LiRkdT606 IdRelS1218 LqRgpS1271
;Q8R3L2	Transcription factor 25	Tcf25	1	6	2,63	2	
Q91WQ3	Tyrosine--tRNA ligase;Tyrosine--tRNA ligase, cytoplasmic;Tyrosine--tRNA ligase, cytoplasmic, N-terminally processed	Yars	1	10	2,62	2	VyRlsS138
Q8K2I2	Coiled-coil alpha-helical rod protein 1	Cchcr1	0	5	2,62	2	VeRmsT401 VaRipS459
P35456	Urokinase plasminogen activator surface receptor	Plaur	1	4	2,60	2	
Q9QYC0	Alpha-adducin	Add1	1	5	2,59	2	VdRgsT212
P28843	Dipeptidyl peptidase 4	Dpp4	1	5	2,59	2	
Q9R0L6	Pericentriolar material 1 protein	Pcm1	5	30	2,59	2	VgRrrT77 LtReiS378 VsRhiS1432
Q922B9	Sperm-specific antigen 2 homolog	Ssfa2	1	4	2,59	2	LqRigS268 LtRsnT290 LlRtaS502 LpReeS640

Uniprot entry	Protein names	Gene names	Peptides EGFP	Peptides PKD3ca	norm.log2.Ratio. filt.LFQ.intensity	Sig.	Putative PKD substrate motifs
							VdRsqS728 LiReqS1075
G3UWQ7	Protein regulator of cytokinesis 1	Prc1	0	2	2,59	2	LqRelS601
Q8C4X2	Casein kinase I isoform gamma-3	Csnk1g3	0	11	2,58	2	
Q9Z0P5	Twinfilin-2	Twf2	1	4	2,57	2	LfRldS75
P16331	Phenylalanine-4-hydroxylase	Pah	0	9	2,56	2	LsRklS16 IpRpfS411
Q9WVK4	EH domain-containing protein 1	Ehd1	1	6	2,56	2	
Q9Z1M8	Protein Red	Ik	0	5	2,54	2	
P46978	Dolichyl-diphosphooligosaccharide--protein glycosyltransferase subunit STT3A	Stt3a	1	5	2,54	2	VlRfeS43 VdRegS631
P21278	Guanine nucleotide-binding protein subunit alpha-11	Gna11	1	6	2,53	2	VdRiaT169
O70194	Eukaryotic translation initiation factor 3 subunit D	Eif3d	1	5	2,51	2	VqRvgS274 ViRvyS521
P47740	Fatty aldehyde dehydrogenase	Aldh3a2	2	11	2,49	2	
O70479	BTB/POZ domain-containing adapter for CUL3-mediated RhoA degradation protein 2	Tnfaip1	1	7	2,49	2	LtRhdT51 VkRysT302
Q8BG05	Heterogeneous nuclear ribonucleoprotein A3	Hnrnpa3	0	5	2,46	2	VsRedS94
Q8BJ64	Choline dehydrogenase, mitochondrial	Chdh	2	3	2,44	2	VsRgkT196
P24456	Cytochrome P450 2D10	Cyp2d10	3	10	2,42	2	LpRitS382
Q9WV55	Vesicle-associated membrane protein-associated protein A	Vapa	1	7	2,41	2	
B7ZMP1	Probable Xaa-Pro aminopeptidase 3	Xpnpep3	1	3	2,41	2	LqRryS32
P28656	Nucleosome assembly protein 1-like 1	Nap1l1	1	6	2,40	2	
Q9QXG4	Acetyl-coenzyme A synthetase, cytoplasmic	Acss2	0	3	2,40	2	
Q91VH2	Sorting nexin-9	Snx9	1	9	2,39	2	IqRgnS194 VkRvgT543
P18406	Protein CYR61	Cyr61	1	10	2,39	2	IcRaqS95
Q9DAW6	U4/U6 small nuclear ribonucleoprotein Prp4	Prpf4	2	6	2,38	2	
Q8BP47	Asparagine--tRNA ligase, cytoplasmic	Nars	2	6	2,38	2	VlRdgT164 LeRflS536
Q9R0H0	Peroxisomal acyl-coenzyme A oxidase 1	Acox1	3	13	2,37	2	
P24549	Retinal dehydrogenase 1	Aldh1a1	3	15	2,35	2	
Q64458	Cytochrome P450 2C29	Cyp2c29	2	9	2,33	2	LwRqsS24 VgRhrS336
P61967	AP-1 complex subunit sigma-	Ap1s1	0	3	2,31	2	

Uniprot entry	Protein names	Gene names	Peptides EGFP	Peptides PKD3ca	norm.log2.Ratio. filt.LFQ.intensity	Sig.	Putative PKD substrate motifs
	1A						
P16406	Glutamyl aminopeptidase	Enpep	1	8	2,28	2	ViRyiS849 LgRivT885
Q922M3	BTB/POZ domain-containing adapter for CUL3-mediated RhoA degradation protein 3	Kctd10	2	12	2,27	2	
Q62433	Protein NDRG1	Ndrg1	7	10	2,11	2	LmRsrT328
P62960	Nuclease-sensitive element-binding protein 1	Ybx1	7	20	2,00	2	InRndT78
Q99JB8	Protein kinase C and casein kinase II substrate protein 3	Pacsin3	4	19	2,61	1	
Q9QXZ0	Microtubule-actin cross-linking factor 1	Macf1	15	56	2,47	1	LeRekS418 IkRkyT814 VfRskT854 IeRnqT1331 IdRqvT1767 LkRqgS3889 IsRqkS4129 LeRrwT5394 LsRgdS6362 IeRgrS6501
Q9CY66	H/ACA ribonucleoprotein complex subunit 1	Gar1	2	3	2,26	1	
P60766	Cell division control protein 42 homolog	Cdc42	0	3	2,25	1	
Q9DB77	Cytochrome b-c1 complex subunit 2, mitochondrial	Uqcrc2	4	10	2,18	1	LsRagS9 LlRlaS87
Q03963	Interferon-induced, double-stranded RNA-activated protein kinase	Eif2ak2	0	4	2,11	1	
Q99N93	39S ribosomal protein L16, mitochondrial	Mrpl16	1	3	2,07	1	
QQ80YE7	Death-associated protein kinase 1	Dapk1	1	9	2,04	1	IeRevS66 LsRkaS289 VsRrdS1433
P68368	Tubulin alpha-4A chain	Tuba4a	7	18	2,01	1	LnRliS232
P42932	T-complex protein 1 subunit theta	Cct8	5	18	1,97	1	LvRlnS317 VlRgsT381
Q9D0M3	Cytochrome c1, heme protein, mitochondrial	Cyc1	3	4	1,96	1	
P50544	Very long-chain specific acyl-CoA dehydrogenase, mitochondrial	Acadvl	2	17	1,93	1	LpRvaS208
Q9DBG6	Dolichyl-diphosphooligosaccharide--protein glycosyltransferase subunit 2	Rpn2	0	5	1,91	1	LdRpfT46
Q8C7U1	NEDD4-binding protein 3	N4bp3	0	6	1,91	1	
O88967	ATP-dependent zinc metalloprotease YME1L1	Yme1l1	0	6	1,91	1	
E9Q555	E3 ubiquitin-protein ligase	Rnf213	8	24	1,90	1	IhRggS427

Uniprot entry	Protein names	Gene names	Peptides EGFP	Peptides PKD3ca	norm.log2.Ratio. filt.LFQ.intensity	Sig.	Putative PKD substrate motifs
	RNF213						LdRifS511 LfRtwT1602 LrRclT1845 IlRleS2501 VlRnfS2949 LyRkvS3210 LsRmgS3384 LlRdaS4057 LvRklS4233 LtRllT4537 LlRvqS4605 IqRqiS4908
Q8CD15	Bifunctional lysine-specific demethylase and histidyl-hydroxylase MINA	Mina	2	9	1,90	1	VcRsiS107 VtRklS309
Q99L45	Eukaryotic translation initiation factor 2 subunit 2	Eif2s2	4	16	1,89	1	VvRvgT212
Q3TGW2	Endonuclease/exonuclease/phosphatase family domain-containing protein 1	Eepd1	3	8	1,87	1	IpRdpS16 VfRlaT265
Q8R0X7	Sphingosine-1-phosphate lyase 1	Sgpl1	2	14	1,87	1	
P97449	Aminopeptidase N	Anpep	12	28	1,87	1	ViRmlS487 VnRppT745 LnRylS845 VtRrfS909
P19157	Glutathione S-transferase P 1	Gstp1	2	7	1,86	1	
Q6R0H7	Guanine nucleotide-binding protein G(s) subunit alpha isoforms XLas	Gnas	5	15	1,84	1	LpRshT699
Q640L3	Cell cycle progression protein 1	Ccpg1	2	3	1,82	1	LeRcwT286
P80318	T-complex protein 1 subunit gamma	Cct3	6	25	1,81	1	IsRwsS170 LlRgaS380
P49813	Tropomodulin-1	Tmod1	2	11	1,80	1	
Q8JZQ9	Eukaryotic translation initiation factor 3 subunit B	Eif3b	2	5	1,77	1	VeRrrT741
O70589	Peripheral plasma membrane protein CASK	Cask	1	5	1,75	1	LkReaS64 LkRilT433 IhRqgT539
Q9CPR4	60S ribosomal protein L17	Rpl17	3	15	1,75	1	
P09411	Phosphoglycerate kinase 1	Pgk1	3	10	1,74	1	
O09167	60S ribosomal protein L21	Rpl21	6	7	1,71	1	
Q69ZX8	Actin-binding LIM protein 3	Ablim3	3	11	1,67	1	LhRtpS598 LeRhlS649
P10126	Elongation factor 1-alpha 1	Eef1a1	6	15	1,67	1	VgRveT269
Q80TP3	E3 ubiquitin-protein ligase UBR5	Ubr5	8	29	1,66	1	LsRlgS293 LyRllT1254 LrRsgT1751 LaRayS1783

Uniprot entry	Protein names	Gene names	Peptides EGFP	Peptides PKD3ca	norm.log2.Ratio. filt.LFQ.intensity	Sig.	Putative PKD substrate motifs
							ViRqiS1790 LeRkrT1971
P11983	T-complex protein 1 subunit alpha	Tcp1	6	18	1,63	1	
Q0P678	Zinc finger CCCH domain-containing protein 18	Zc3h18	3	4	1,62	1	
Q9DB20	ATP synthase subunit O, mitochondrial	Atp5o	2	7	1,60	1	
Q3UQ44	Ras GTPase-activating-like protein IQGAP2	Iqgap2	3	14	1,59	1	LdRkqS554 LkRknS1458
P62082	40S ribosomal protein S7	Rps7	4	14	1,53	1	
P63037	DnaJ homolog subfamily A member 1	Dnaja1	3	11	1,52	1	
Q64339	Ubiquitin-like protein ISG15	Isg15	4	6	1,50	1	
Q91YD6	Villin-like protein	Vill	7	14	1,49	1	
Q99K51	Plastin-3	Pls3	8	18	1,48	1	LkRaeS339 LmRryT506 VnRtlS533
P17225	Polypyrimidine tract-binding protein 1	Ptbp1	5	14	1,48	1	
P06151	L-lactate dehydrogenase A chain	Ldha	4	10	1,48	1	
Q62191	E3 ubiquitin-protein ligase TRIM21	Trim21	6	17	1,46	1	LeRsgS260
O08749	Dihydrolipoyl dehydrogenase, mitochondrial	Dld	2	9	1,46	1	
P26041	Moesin	Msn	8	21	1,45	1	
Q8VI94	2-5-oligoadenylate synthase-like protein 1	Oasl1	8	20	1,45	1	VlRstT80
Q4U2R1	E3 ubiquitin-protein ligase HERC2	Herc2	22	54	1,42	1	VyRakS97 LaRvgS198 LqRfqS347 LdRlaT406 LgRggS643 LlRqvS811 VaRriS1036 LlResT2123 LkRchS2773

Uniprot entry	Protein names	Gene names	Peptides EGFP	Peptides PKD3ca	norm.log2.Ratio. filt.LFQ.intensity	Sig.	Putative PKD substrate motifs
							LiRkkT2949 IpRqiT3041 LgRggS3191 VnRkpT3302 VnRivS3668 LrRllT3785 LgRggS4184 VkRsrS4432
P62858	40S ribosomal protein S28	Rps28	2	3	1,40	1	LgRtgS23
Q99KP6	Pre-mRNA-processing factor 19	Prpf19	2	11	1,36	1	
P46735	Unconventional myosin-Ib	Myo1b	78	83	1,34	1	LeRdfS230 LeRafS325 LyRdlS539 LkRppT569
…							
Q9EP53	Hamartin	Tsc1	6	16	0,71	0	LfRnkS1094